Supplementary Information

Fast and Stable Charge Transfer at Lithium-Sulfide (Electrolyte) Interface via In-Situ Solidified Li^+-Conductive Interlayer

Ya-Hui Wang[a,b], Xu-Sheng Zhang[a,b], Cai-Cai Li[a,b], Hao Zeng[a,e], Zhe Chen[c], Liang Zhang[d], Jin-Chi Zheng[d], Yuan Luo[d], Sen Xin[a,b,*], Yu-Guo Guo[a,b]

[a] CAS Key Laboratory of Molecular Nanostructure and Nanotechnology, CAS Research/Education Center for Excellence in Molecular Sciences, Beijing National Laboratory for Molecular Sciences (BNLMS), Institute of Chemistry, Chinese Academy of Sciences (CAS), Beijing 100190, China;

[b] University of Chinese Academy of Sciences, Beijing 100049, China

[c] College of Environmental Science and Engineering, North China Electric Power University, Beijing, 102206, China.

[d] State Grid Xinjiang Company Limited Electric Power Research Institute, Xinjiang, 830013, China.

[e] Williston Northampton School, Easthampton, Massachusetts, 01027, United States.

Experimental section

Preparation of glassy $75Li_2S$-$25P_2S_5$ (LPS) electrolyte powder

A certain amount of lithium sulfide (Li_2S, Alfa Aesar, 99.9%) and phosphorus pentasulfide (P_2S_5, Macklin, 99%) was weighed according to the molar ratio of 75:25, placed in an agate mortar and hand-milled for 30 minutes, then poured into a ball mill jar for high-energy ball milling (Argon atmosphere 500 rpm) for 20 hours.

Preparation of precursor solution of Li^+-conductive interlayer (LCI)

The precursor solution of LCI was made by dissolving 2 mol L^{-1} lithium hexafluorophosphate ($LiFP_6$; Alfa Aesar, 98%) and 1 mol L^{-1} bis(trifluoromethane)sulfonimide lithium salt (LiTFSI; Sigma-aldrich 99.95% trace metals basis) into a 1, 3-dioxolane (DOL; Alfa Aesar, 99.5%, stab.) and 1, 2-dimethoxyethane (DME) (Alfa Aesar, 99+%) solvent (1:1, v/v) mixture. The decomposition of $LiFP_6$ triggers the ring-opening cationic polymerization of DOL monomer and thereby converting the precursor solution into LCI. All the preparation processes were conducted in an argon-filled glovebox (O_2< 0.1 ppm, H_2O < 0.1 ppm).

Assembly of symmetrical Li|LPS|Li, Li|LPS|SS, and blocking SS|LPS|SS batteries

About 150 mg of LPS powder was weighed and put into a homemade mold with a diameter of 10 mm and then cold pressed under 360 MPa for 5 minutes. And the Li foils (Φ12) were placed on both sides of LPS pellet followed by cold pressing under 100 MPa for 3 minutes. Similarly, the assembly of Li|LPS|SS and blocking SS|LPS|SS cells was the same as above, except that the corresponding Li foils were replaced by stainless steels. All the assembled processes were conducted in an argon-filled glovebox (O_2 < 0.1 ppm, H_2O < 0.1 ppm).

Assembly of symmetrical Li|LCI-LPS-LCI|Li batteries

About 80 mg of LPS powder was weighed and put into a homemade mold with a diameter of 10 mm and then cold pressed under 360 MPa for 5 minutes. After that, 10 μL precursor solution was injected into the interface between LPS pallet and Li foil. Subsequently, the assembled batteries were left to stand for a period of time to form LCI completely inside the battery. All the assembled processes were conducted in an argon-filled glovebox (O_2 < 0.1 ppm, H_2O < 0.1 ppm).

Materials characterization

The X-ray diffraction (XRD) patterns were collected on a Bruker D8 Advance diffractometer with Cu Kα radiation (λ = 1.5418 Å) in the 2θ range from 10° to 80° by using a sealed container to avoid oxygen. The Fourier Transform Infrared (FTIR) spectrum of the prepared LCI was recorded using VERTEX 70v in the range of 400 to 4000 cm^{-1} to investigate the functional group of LCI. The morphology and element mapping were characterized by REGULUS SU8100 scanning electron microscopy (SEM) with an energy-dispersive X-ray spectroscopy (EDS) system. X-ray photoelectron spectroscopy (XPS) was recorded on AXIS Supra electron spectrometer using 150 W Al Kα radiation ($h\nu$ = 1486.6 eV).

Electrochemical measurements

Electrochemical impedance spectroscopy (EIS) measurements were investigated over the frequency range from 1 MHz to 0.1 Hz with an amplitude of 10 mV on a Princeton PARSTAT MC 1000 multi-channel electrochemical workstation. The ionic conductivity σ was calculated based on the following equation,

$$\sigma = \frac{L}{R_{SSE} \times S}$$

where L is the thickness of electrolytes, R_{SSE} is the resistance according to the EIS measurement, S is the effective contact area between the electrolyte and stainless steel.

The activation energy ($E_{a(SSE)}$) of the electrolyte was obtained according to the Arrhenius equation.

$$\sigma = \frac{A}{T} exp(\frac{-E_a}{K_B T})$$

where, σ (S cm^{-1}) is the ionic conductivity of the electrolyte, A is the pre-exponential factor, T (K) is the thermodynamic temperature, K_B (1.38×10^{23} J K^{-1}) is the Boltzmann constant, Ea (J mol^{-1}) is the activation energy of the electrolyte.

In the temperature range of 0-80 °C, the ionic conductivity of the electrolyte was tested every 10 °C as an interval. The relationship between the ionic conductivity and temperature was drawn according to the Arrhenius equation, and the slope is $E_{a(SSE)}$.

The galvanostatic polarization and cycling measurements were conducted using a LAND battery test system (LANHE Inc. CT2001A). Galvanostatic cycling performance of Li|Li cells were tested with current density 0.1 mA cm^{-2} corresponding to areal capacity of 0.1 mAh cm^{-2}. For the critical current density tests, the initial current density is 0.1 mA cm^{-2}, the deposited capacity is 0.1 mAh cm^{-2}. After that, Li plating and stripping was tested at a fixed capacity of 0.1 mAh cm^{-2} but a step-increased current density from 0.1 mA cm^{-2} to 5 mA cm^{-2}.

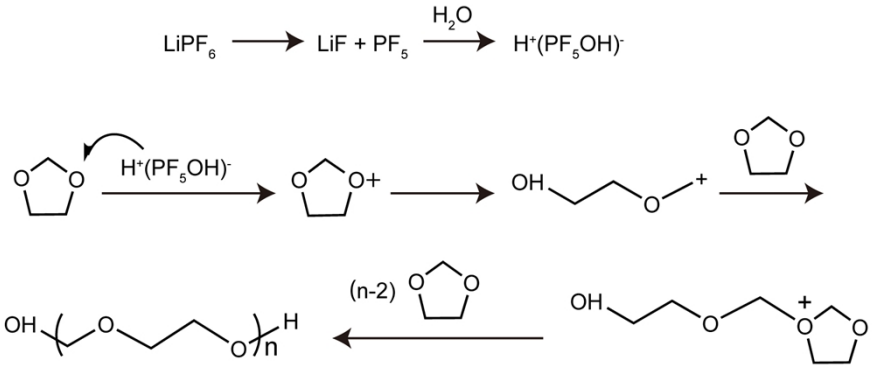

Figure S1. The polymerization mechanism of LCI.

Table S1. The specific values of resistances and the calculation result of ionic conductivity of Figure 2C.

	Thickness (cm)	Effective area (cm^2)	R_{SSE} (Ω)	Ionic conductivity ($mS\ cm^{-1}$)
LPS	0.295	1.13	933	0.28
LPS/LCI	0.310	1.13	671	0.41

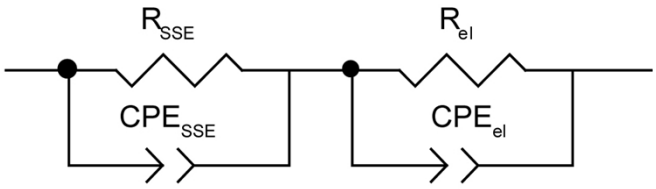

Figure S1. Detailed equivalent circuit of Figure 2C, where R_{SSE} is the resistance of LPS powder and R_{el} is the resistance of blocking electrode. Each constant phase element (CPE) describes the capacitance of the corresponding process.

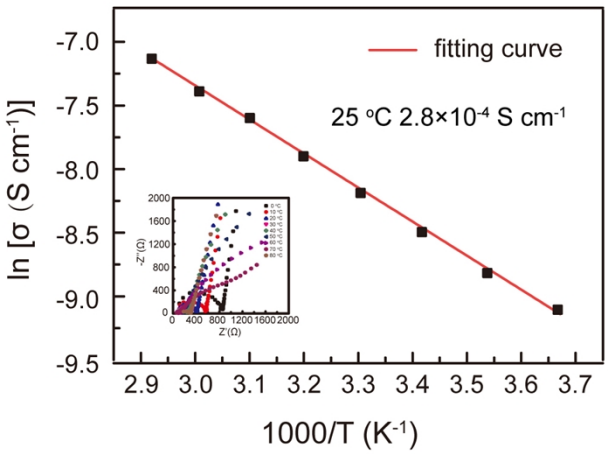

Figure S2. Arrhenius curve of ionic conductivity of glassy $75Li_2S$-$25P_2S_5$ electrolyte; Inset: EIS spectra of glassy$75Li_2S$-$25P_2S_5$ electrolyte at different temperatures.

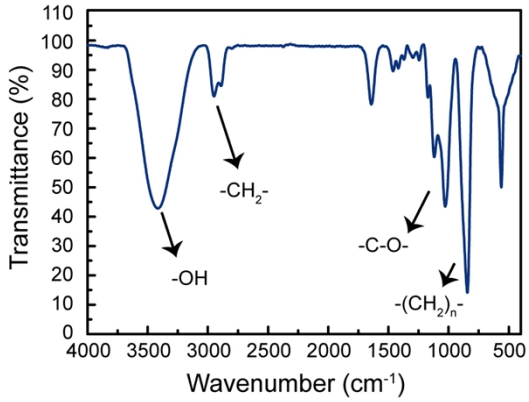

Figure S3. FTIR spectrum of LCI.

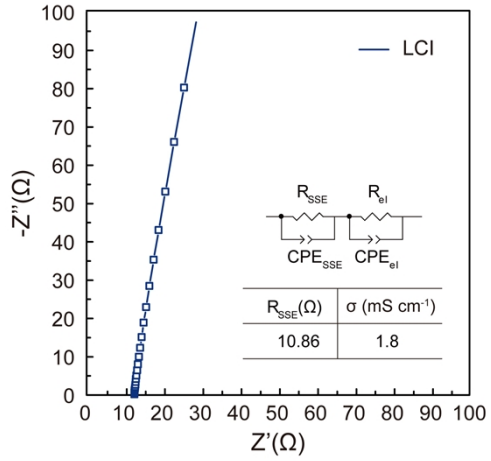

Figure S4. EIS spectrum of LCI.

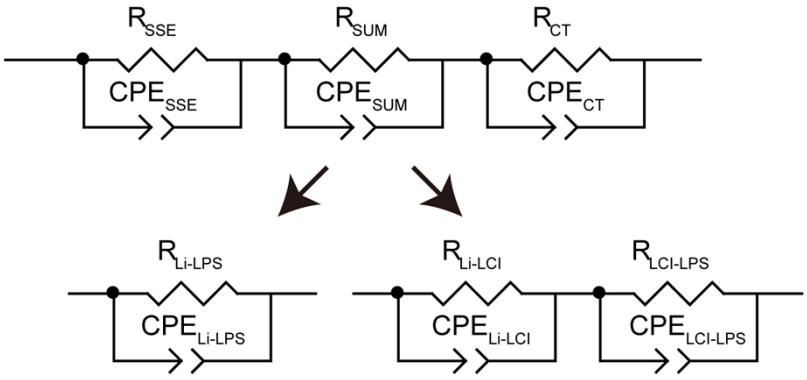

Figure S5. Detailed equivalent circuit of Figure 4c, d, where R_{SSE} is the resistance of LPS, R_{Li-LPS}, R_{Li-LCI}, $R_{LCI-LPS}$ is the Li/LPS, Li/LCI, LCI/LPS interphase resistance, respectively. R_{CT} is the electrochemical transfer polarization resistance of Li plating/stripping. Each constant phase element (CPE) describes the capacitance of the corresponding process.

Table S2. The specific values of resistances in Figure S6.

	R_{sse} (Ω)	R_{SUM} (Ω)	R_{CT} (Ω)
Li|LPS|Li Before cycle	298.9	178.2	149.5
Li|LPS|Li After 30 cycles	-	-	-
Li|LCI-LPS-LCI|Li Before cycle	303.3	92.4	208.2
Li|LCI-LPS-LCI|Li After 30 cycles	301.4	184.5	168.3

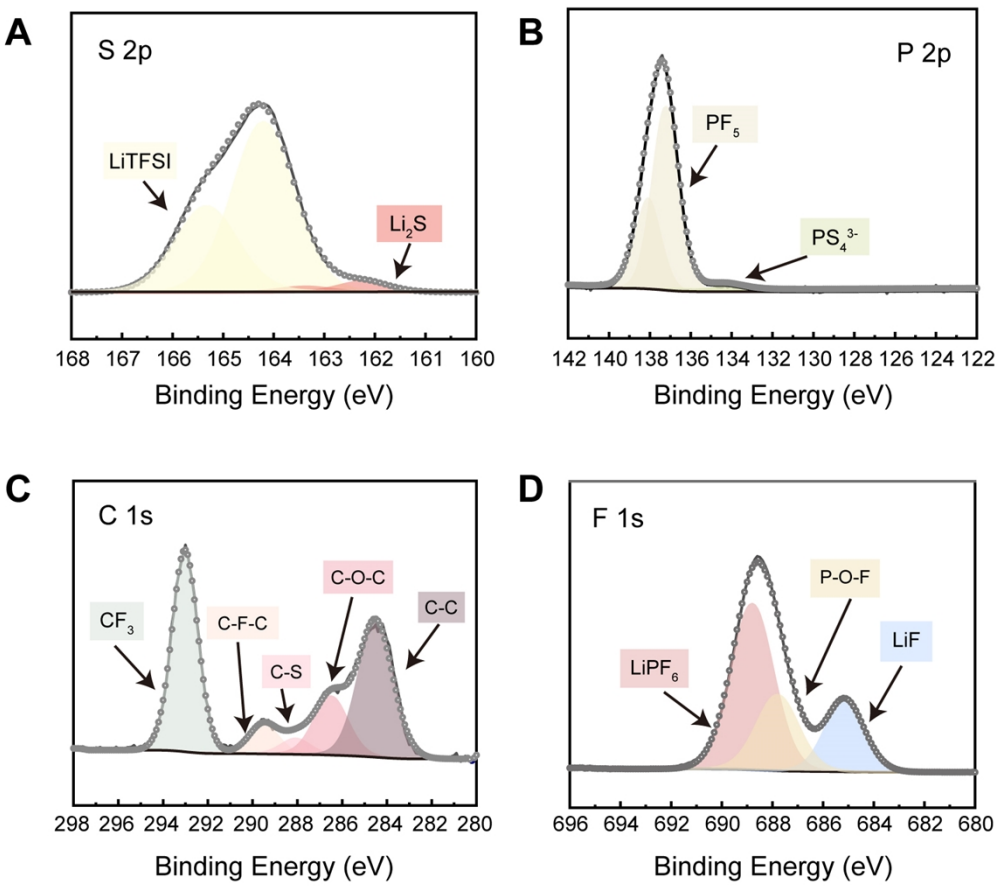

Figure S6. XPS spectrum of the Li anode recovered from Li|LCI-LPS-LCI|Li battery before cycing.

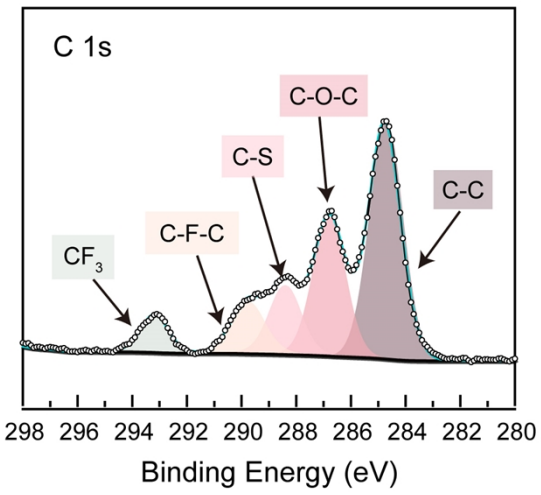

Figure S7. C 1s XPS spectrum of the cycled Li anode recovered from Li|LCI-LPS-LCI|Li battery. The battery is tested for 30 cycles at a current density of 0.1 mA cm^{-2} for 0.1 mAh cm^{-2}

at room temperature.

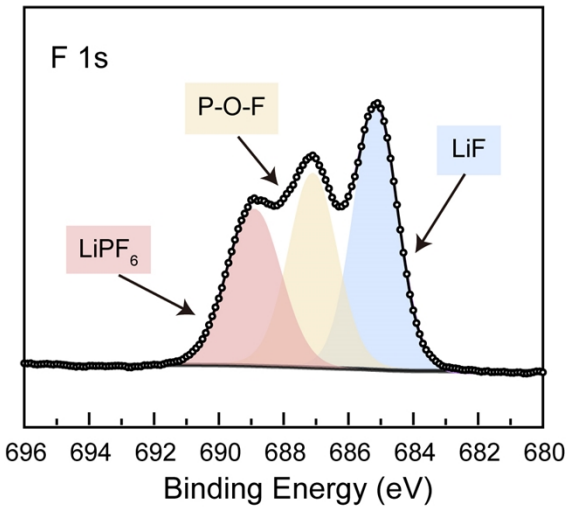

Figure S8. F 1s XPS spectrum of the cycled Li anode recovered from Li|LCI-LPS-LCI|Li battery. The battery is tested for 30 cycles at a current density of 0.1 mA cm^{-2} for 0.1 mAh cm^{-2} at room temperature.

Table S3. XPS binding energies with attributed species shown in Figure 5, S8.

Spectra details	Binding energy (eV)		Attributed species
P 2p	131.70	132.57	$P_2S_7^{4-}$
	134.19	135.06	PS_4^{3-}
	137.05	137.92	PF_5
	125.82	126.69	Li_3P
S 2p	163.02	164.18	LiTFSI
	161.56	162.72	PS_4^{3-}
	159.85	161.01	Li_2S

Table S4. XPS binding energies with attributed species shown in Figure S6, S7, S8.

Spectra details	Binding energy (eV)	Attributed species
C 1s	284.77	C-C
	286.79	C-O-C
	288.40	S-C
	289.78	C-F-C
	293.19	CF_3
F 1s	685.13	LiF
	687.10	P-O-F
	688.95	$LiPF_6$